

UCLA

UCLA Electronic Theses and Dissertations

Title

Vertebral Implantation of NELL-1 Enhances Bone Formation in Osteoporotic Sheep

Permalink

<https://escholarship.org/uc/item/69p2d5wf>

Author

Chiang, Michael Ming-Ying

Publication Date

2013

Peer reviewed|Thesis/dissertation

UNIVERSITY OF CALIFORNIA

Los Angeles

Vertebral Implantation of NELL-1
Enhances Bone Formation in Osteoporotic Sheep

A thesis submitted in partial satisfaction
of the requirements for the degree
Master of Science in Oral Biology

By

Michael Ming-Ying Chiang

2013

© Copyright by
Michael Ming-Ying Chiang
2013

ABSTRACT OF THESIS

Vertebral Implantation of NELL-1 Enhances Bone Formation In Osteoporotic Sheep

By

Michael Ming-Ying Chiang

Master of Science in Oral Biology

University of California, Los Angeles, 2013

Professor Shen Hu, Co-Chair

Professor Xinli Zhang, Co-Chair

Background: Vertebral compression fractures related to osteoporosis greatly afflict the aging population. The most commonly used therapy today is balloon kyphoplasty, a procedure that involves the inflation of a balloon and injection of cement such as polymethyl methacrylate. However, this treatment is far from ideal as it is associated with significant side effects, including local toxicity and rare systemic complications. NELL-1, a secreted osteoinductive factor that possesses both pro-osteogenic and anti-resorptive properties, is a promising candidate for an alternative to current treatment modalities. The use of NELL-1 in balloon kyphoplasty might improve post surgical outcome for over 10 million osteoporotic American who are susceptible to vertebral

compression fractures. The present study utilizes the pro-osteogenic properties of recombinant human NELL-1 (rhNELL-1) in lumbar spine balloon kyphoplasty using an osteoporotic sheep model.

Methods: Osteoporosis in N=8 sheep was induced through ovariectomy, dietary depletion of calcium and vitamin D, and steroid administration. After osteoporotic induction was confirmed by dual-energy X-ray absorptiometry (DXA), balloon kyphoplasty was performed in N=6 sheep with significant osteopenia. Sheep were randomly implanted with the control vehicle, comprised of hyaluronic acid (HA), hydroxyapatite, and β -tricalcium phosphate (β -TCP), or the treatment material of rhNELL-1 protein lyophilized onto β -TCP mixed with HA. Analysis of lumbar spine healing was performed by radiographic, histologic, and biomechanical testing.

Results: rhNELL-1 treatment significantly increased lumbar spine bone formation, as determined by bone mineral density, fractional bone volume, and mean cortical width by micro-computed tomography. Histological analysis revealed a significant increase in bone area as well as osteoblast number and decrease in osteoclast number around the implant site. Biomechanical properties of trabecular bone were analyzed using Finite Element Analysis (FEA), demonstrating that rhNELL-1-treatment resulted in a significantly more stress-resistant composition.

Conclusion: Our findings suggest rhNELL-1-based balloon kyphoplasty successfully improved cortical and cancellous bone regeneration in the lumbar spine of osteoporotic sheep. Thus, rhNELL-1 based balloon kyphoplasty represents a potential new anabolic, anti-resorptive local therapy for treating osteoporotic bone loss and/or fractures.

The thesis of Michael Ming-Ying Chiang is approved.

Sotirios Tetradis

Xinli Zhang, Committee Co-Chair

Shen Hu, Committee Co-Chair

University of California, Los Angeles

2013

This thesis is dedicated to

Dr. Ting, Dr. Soo, and Dr. Zhang for all their academic guidance
and my parents Linus and Catherine
who have supported me throughout my life.

In addition I would like to dedicate this work to
my co-workers in the lab,
my fellow residents in the Orthodontic program,
and all my friends.

TABLE OF CONTENTS

List of Figures	vii
Introduction.....	1
Materials and Methods.....	9
Results.....	14
Discussion.....	30
References.....	33

LIST OF FIGURES

Figure 1	Balloon kyphoplasty surgery for treatment of vertebral compression fractures.....	4
Figure 2	<i>NELL-1</i> gene and NELL-1 protein putative domains.....	5
Figure 3	Hypothetical model of the effects of NELL-1 on osteochondral differentiation.....	7
Figure 4	Induction of osteoporosis in sheep.....	16
Figure 5	rhNELL-1 implant material contents and bi-level sheep balloon kyphoplasty surgery group.....	17
Figure 6	BMD quantification of sheep lumbar vertebrae post-implantation.....	18
Figure 7	MicroCT analysis of sheep lumbar vertebrae.....	19, 21
Figure 8	Histological analysis of sheep lumbar vertebrae.....	23, 25
Figure 9	Osteoblast and Osteoclast numbers in the peri-implant bone tissue	27
Figure 10	Finite Element Analysis of peri-implant trabecular bone	29

Acknowledgements

This work was supported by the CIRM Early Translational II Research Award TR2-01821, NIH/NIDCR (grants R21 DE0177711 and RO1 DE01607), and T32 training fellowship (5T32DE007296-14) to A.W.J.

Drs. X.Z., K.T., and C.S. are inventors of Nell-1 related patents. Drs. X.Z., K.T., and C.S are founders of Bone Biologics Inc., which sublicenses Nell-1 patents from the UC Regents, which also hold equity in the company.

Vertebral Implantation of NELL-1 Enhances Bone Formation In Osteoporotic Sheep

INTRODUCTION

Vertebral compression fracture (VCF's) of the thoracolumbar spine affects approximately 1.5 million people annually in the United States, especially in the elderly population (1). Osteoporosis, the most common disease of bone, is responsible for approximately 700,000 vertebral compression fractures (VCF) in the United States annually (2), comprising half of the nation's annual VCF. Further, the annual cost of osteoporotic fractures in the United States is estimated to be greater than \$5-10 billion (2). The most affected population are the postmenopausal women, whom 25% suffer from vertebral fractures (3). Due to an aging United States and world population, annual costs for osteoporotic fractures are projected to increase four-fold by 2040 (2). Nonetheless, approximately \$746 million is spent annually for vertebral fractures in the United States (3).

Untreated VCF can cause debilitating back pain, spinal deformity, disability, reduction of respiratory function, and increase the risk of death (4-8). Due to the physical and functional consequences, a significant decrease in the quality of life of vertebral fractured patients is expected. Moreover, this disease can impair ones social function and interaction, which in turns contribute to development of severe depression (9). In summary, vertebral compression fracture possess an immense biomedical burden, and effect not only the biological aspect of a patient, but further also are detrimental to a

patient's psyche.

In osteoporotic vertebral compression fractures, age-related bone loss results from diminished bone formation and inappropriate bone resorption by underproduction of osteoblasts and overproduction of osteoclasts (11). In addition, aging decreases expression of osteoblast specific transcription factors, such as Runx2 and Dlx5, in aged mesenchymal marrow stem cells (mMSC) and increases expression of adipocyte specific transcription factor PPAR γ 2, in aged mMSC. Both factors contribute to the development of osteoporotic vertebrae by increasing the number of mMSC-derived adipocytes and decreasing the number of mMSC-derived osteoblasts (10). The increase in the mMSC-derived adipocytes to mMSC-derived osteoblasts ratio creates an unfavorable conditions for bone stem cell participation in fracture repair and commonly lead to failure in healing osteoporotic fractures (11). Consequently, it is crucial to investigate methods of preventing and healing VCF in osteoporotic patients.

Balloon kyphoplasty is a minimally invasive surgical procedure performed to relieve back pain, increase function and improve quality of life after VCF (12). Kyphoplasty involves the inflation of a balloon in the vertebral body, followed by the injection of cement such as polymethyl methacrylate (PMMA) into the space created by the balloon (13). (**Figure 1**) From recent studies, balloon kyphoplasty with polymethyl methacrylate (PMMA) results in significant improvements in patients' quality of life, functionality, and overall reduction in pain in comparison to non-surgical treatments (14,15). Studies have shown patients treated with balloon kyphoplasty have increased vertebral height,

functional capacities, and a significant improvement in Visual Analog Scale (VAS) pain measurements (15). However, current PMMA cement-based VCF therapies have significant disadvantages including cellular toxicity and potential for neural damage caused by an acute exothermic reaction during polymerization of the PMMA (16). Furthermore, cement from the fracture site can leak, and in rare cases cause embolization and death (17). In addition, long-term complications can arise due to differences in the stiffness of cement and bone, predisposing the patient to adjacent fractures or re-fractures of the cement-treated vertebrae (18). Moreover, PMMA cement-based VCF therapies may permanently exclude and eliminate mMSC from the vertebral bone marrow space due to cellular toxicity, thus hampering endogenous bone healing. Due to the safety concerns of PMMA cements, Calcium Phosphate Cement (CPC) has been used as an alternative. However, CPC induces ectopic bone formation (19), and heterotopic ossification, which alters the normal biomechanics and results in subsequent VCFs (20).

Nel-like molecule-1 (NELL-1) is a novel secreted osteogenic differentiation factor, first identified to have osteoinductive properties by its overexpression in craniosynostosis patients (21). NELL-1 is a secreted protein comprised of 810 amino acids with a molecular weight of about 90 kDa before N-glycosylation and oligomerization (21). It contains several structural motifs, including a secretory signal peptide, a thrombospondin-1 (TSP-1)-like module (TSPN, overlapping with a laminin G domain), four chordin-like, cysteine-rich (CR) domains and six epidermal growth factor (EGF)-like domains (21). **(Figure 2)**

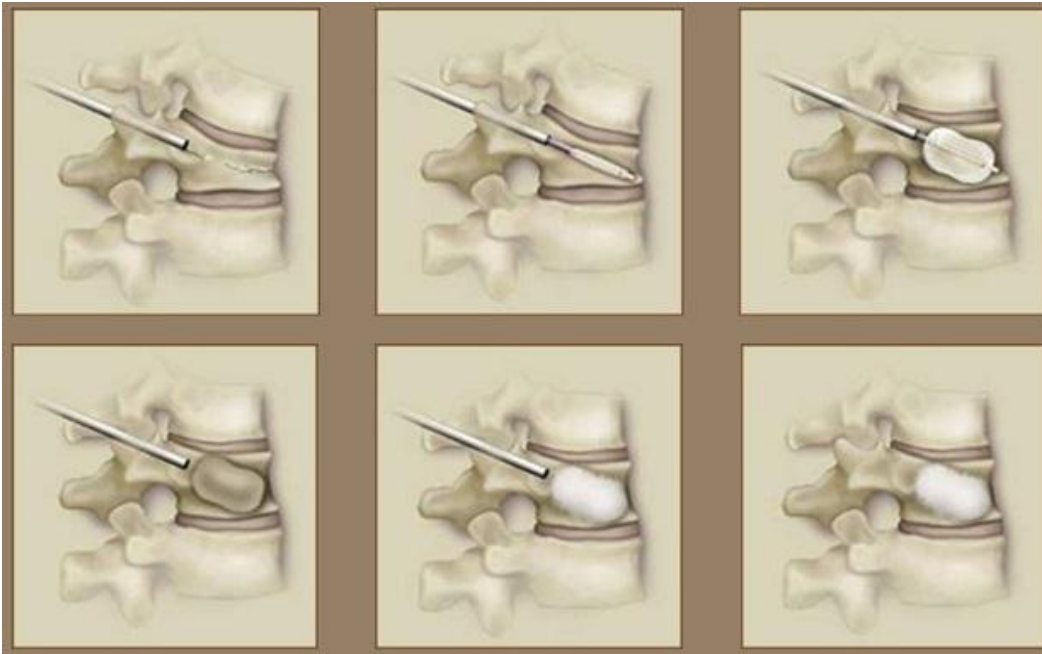


Figure 1. Balloon kyphoplasty surgery for treatment of vertebral compression fractures. A needle is inserted and then a balloon into the fractured and compressed vertebra. The balloon is inflated till the compressed, wedge shaped vertebral body changes to normal cylindrical shape. The balloon is then removed and the vacant space in the vertebra is filled with bone cement. Thus the vertebra becomes normal in shape and the patient gets permanent relief from pain caused by fractured vertebra. Adapted from **Balloon Kyphoplasty for Vertebral Wedging**, Retrieved November 22, 2013, from http://thespineclinic.in/facilities_ballon.php. Copyright 2012 by The Spine Clinic.

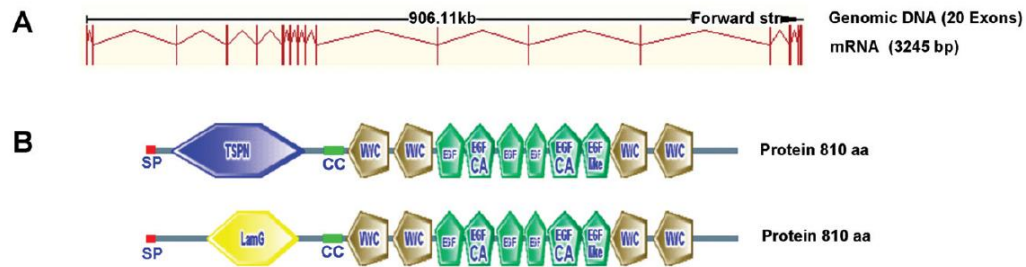


Figure 2. *NELL-1* gene and *NELL-1* protein putative domains.

(A) *NELL-1* has been mapped to 11p15.1-p15.2 and spans about 906 kb with 20 exons coding for a major transcript of 3.245 kb. (B) *NELL-1* contains several putative domains predicted by SMART, with some modifications. At its NH₂-terminal, it appears to have two different modules: an NH₂-terminal thrombospondin-1-like module (TSPN) (top) or a laminin G domain (LamG) (bottom). A coiled-coil region (CC) is in between the N-terminal domain and other major domains, which include four von Willebrand factor type C (vWC), three epidermal growth-factor-like (EGF), two calcium-binding EGF (EGF-CA), and an unclassified EGF-like (EGF-like) domain. A signal peptide (SP) that does not meet SMART scores with high confidence is also displayed. Adapted from "The Role of *NELL-1*, a Growth Factor Associated with Craniosynostosis, in Promoting Bone Regeneration," by X. Zhang and J. Zara, 2010, *J DENT RES*, 89: 865. Adapted with permission

Previously, NELL-1 has been observed to stimulate bone regeneration via endochondral or intramembranous ossification, i.e. with or without a cartilage intermediate (21). In addition, NELL-1 has been demonstrated to induce significant bone formation in calvarial, axial, and appendicular defects, in both small and large animal models (22-26). Currently, Bone Morphogenetic Protein 2 (BMP2) is the gold standard substitute for autogenous bone. Although causing significant bone formation, it is also associated with multiple clinical complications such as soft-tissue swelling, ectopic bone formation and inflammation (27-34). In contrast, NELL-1 is an osteoblast specific growth factor, capable of suppressing BMP2-induced side effects of cystic bone formation and inflammation (35). Moreover, NELL-1 directly represses adipogenic differentiation (36) and osteoclastogenesis (*manuscript in submission*). Mechanistically, NELL-1 is known to have multiple effects including regulation of Runt-related transcription factor-2 (Runx2) activity and phosphorylation (37), positive regulation of MAPK signaling (38) and induction of Hedgehog signaling pathways (36). NELL-1 is under direct transcriptional regulation of Runx2, and NELL-1 is a functional mediator of Runx2 control of osteochondral differentiation at a relatively late stage. **(Figure 3)**

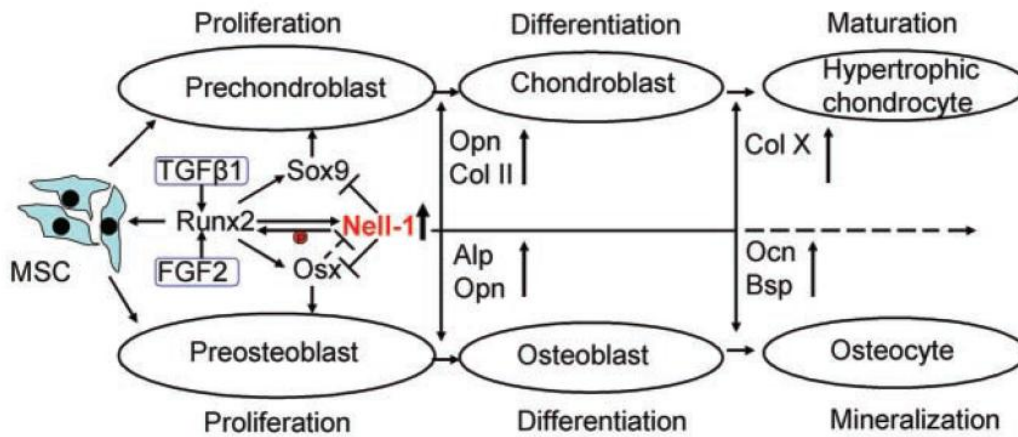


Figure 3. Hypothetical model of the effects of NELL-1 on osteochondral differentiation. NELL-1 is under direct transcriptional regulation of Runx2, and NELL-1 is a functional mediator of Runx2 control of osteochondral differentiation at a relatively late stage. All solid lines represent NELL-1 function suggested by our published data, and the dashed lines represent hypothetical modulation and subjects of ongoing investigation by our laboratory. Adapted from "The Role of NELL-1, a Growth Factor Associated with Craniosynostosis, in Promoting Bone Regeneration," by X. Zhang and J. Zara, 2010, *J DENT RES*, 89: 865. Adapted with permission

In this study, we investigate the therapeutic effects of recombinant human NELL-1 (rhNELL-1) in an osteoporotic sheep model by evaluating healing of the lumbar spine after implantation of rhNELL-1 by balloon kyphoplasty. Sheep were used as they have similarities to humans in terms of spinal dimensions as well as mineral and collagen composition (39). The sheep model is optimal because their vertebral bodies are large enough to accommodate the volume of material necessary to successfully perform balloon kyphoplasty (40). Additionally, sheep are susceptible to osteoporosis with a combined treatment of ovariectomy, steroid administration and dietary deficiency (41). In fact, after a four-month induction period, sheep show resemblance to post-menopausal osteoporotic women (42). Briefly, we found rhNELL-1 balloon kyphoplasty successfully induced an increase in osteoblast and a decrease in osteoclast activity resulting in improved cortical and cancellous bone formation in osteoporotic sheep spine.

MATERIALS AND METHODS

Animal care and ovine osteoporotic induction

Sheep were cared for at Colorado State University according to the Guiding Principles in the Care and Use of Animals (41). Osteoporosis in sheep was induced through ovariectomy (OVX), dietary depletion and steroid administration in eight adult ewes. OVX was performed as previously described (42). Three intramuscular injections of 500 mg methylprednisolone acetate (Depomedrol) were administered at three-week intervals starting two weeks post-OVX. Specifically formulated low calcium and low vitamin D osteoporosis diets (Purina LabDiet) were fed to the sheep for the entire study period (43). Of eight sheep, the six sheep with highest response to osteoporotic induction were used for further study. Response to osteoporotic induction was evaluated by dual-energy X-ray absorptiometry (DXA). A timeline of the study structure including osteoporotic induction, balloon kyphoplasty procedure, and post-operative analyses can be found in Figure 4.

rhNELL-1 implant material preparation

The contents of sheep balloon kyphoplasty implant material can be found in Figure 4. rhNELL-1 implant dosages were used as previously described (26). The control balloon kyphoplasty implant material was 1.5 mL in total volume, composed of hyaluronic acid (HA, 1.1 mL), β -tricalcium phosphate (β -TCP, 150 mg), and hydroxyapatite (1.3 g). β -TCP has been previously shown to increase the biochemical stability and biological efficiency of rhNELL-1 *in vivo* (44). The treatment implant materials was 1.5 mL in total volume, consisted of two dosages of rhNELL-1 protein lyophilized onto β -TCP mixed

into the HA and hydroxyapatite, for sustained protein release (23). The individual components were mixed mechanically before implantation.

Ovine rhNELL-1 balloon kyphoplasty

Surgery was performed four months post-OVX on N=6 osteoporotic sheep. Sheep most responsive to osteoporosis induction were selected for the study. A ventrolateral incision was made for a retroperitoneal approach. Dissection was carried out to expose the lumbar vertebral bodies. Two different vertebral levels were instrumented per sheep (L2 and L4). A 6.0 mm diameter access hole was first drilled in the lateral aspect of the vertebral body. With a Midas Rex bur, a 2.0 cm diameter defect was then created in the central portion of the vertebral body. Next, the woven OptiMesh[®] implant sac was inserted into the vertebral defect. The rhNELL-1 test article was delivered into the mesh bag by impacting a stylet down into the central core with a mallet. Finally, the access hole was covered with bone wax, to prevent leakage. N=3 sheep were randomly assigned to implantation with the control vehicle and N=3 sheep with two doses of the treatment vehicle.

Live ovine radiographic analysis

Dual-energy X-ray absorptiometry (DXA) scans were performed pre- and post-induction of osteoporosis, as well as monthly post-balloon kyphoplasty (Konica Minolta mc5430DL). Bone Mineral Density (BMD) was measured as a result of Bone Mineral Content (g) / Area (cm²).

Post-mortem micro-computed tomography (microCT)

Bone density determination using conventional dual-energy X-ray absorptiometry (DXA) allows assessment of area bone density. It measures the amount of calcium, used as density reference for bone, to determine the amount of bone mass in the area. However, it did not differentiate between cortical and cancellous bone, nor provided a good assessment of bone microarchitecture. High resolution computed tomography (CT) scanner and magnetic resonance imaging (MRI) should be used as a compliment to the DXA to provide insights to the relationship between bone microarchitecture and bone strength (45).

In our study, to better assess the microarchitecture of both cancellous and cortical bone, high resolution, post-mortem microCT scanning and analysis was performed on individual sheep vertebrae. Samples were harvested, fixed with 10% PBS buffered formalin, imaged using high-resolution microCT (Skyscan 1172F, Skyscan, Belgium) at an image resolution of 17.8-18.2 μm and analyzed using Data Viewer, Recon, CTAn, and CTVol softwares provided by the manufacturer. Trabecular analyses were performed on post-mortem individual sheep vertebrae. Trabecular measurements were made using Region of Interests (ROIs) encompassing the entire cancellous bone using CTAn software. All quantitative and structural morphometric data use nomenclature described by the American Society for Bone and Mineral Research (ASBMR) Nomenclature Committee (46).

Histological and histomorphometric analyses

After radiographic analysis, undecalcified histological preparations were performed. Five

micron thick sections were stained with Hematoxylin and Eosin (H&E), Goldner's Modified Trichrome (GMT), and Von Kossa-MacNeal's Tetrachrome. Histologic specimens were analyzed using Olympus BX51 microscopes and images were obtained using MicroFire digital camera with Picture Frame software (Optronics, Goleta, CA). Histomorphometric analysis was completed using Adobe Photoshop CS7. For cortical bone, N=12 random contralateral side fields of implantation were used for analysis. For trabecular bone, four random fields from N=17 specimens were used for analysis. Measurements included percent Trabeculae Area (% Tb. Ar), Cortical Width (Ct. Wi), Trabecular Width (Tb. Wi), Trabecular Number (Tb. N), and Trabecular Spacing (Tb. Sp). Cortical Width was measured on the contralateral side of product implantation. Osteoblast Number (Ob. N) was measured using 200x images of Von Kossa McNeal's Tetrachrome (N=16) stained specimens, whereas Osteoclast Number (Oc. N) was measured using 200x images of GMT staining (N=12). All quantitative and structural morphometric data use nomenclature described by the American Society for Bone and Mineral Research (ASBMR) Nomenclature Committee (46).

Finite Element Analysis (FEA)

To analyze the biomechanical properties of trabecular bone, microCT images were converted to DICOM files using SkyScan Dicom Converter software. Tetrahedral three-dimensional mesh models were created using ScanIP software (Simpleware Limited, Exeter, UK) by drawing a region of interest (ROI) 0.5 mm caudal to the implant site in the midline of the vertebra spanning 5 mm x 5 mm x 10 mm. Finite element analysis (FEA) was performed using ABAQUS software (Dassault Systèmes,

Vézizy-Villacoublay, France). Boundary conditions were set as encastre, constrained in all directions on the lower (caudal) border nodes of the hexahedron. Since similar biomechanical properties are shared between human and sheep vertebral bodies, (47) we applied a uniform compressive stress of 0.5 MPa on the superior surface of the spine, to reproduce human intradiscal pressure experienced in relaxed standing. Finally, the resulting strain energy and tensile strength were analyzed (48).

Statistical analysis

Statistical analysis was performed using an appropriate Student's *t*-test when two values were being compared. When more than two groups were compared, a one-way ANOVA followed by a post-hoc Tukey's test was used for pair-wise comparisons of groups. * $p < 0.05$ and ** $p < 0.01$ were considered to be significant.

RESULTS

Successful induction of sheep osteoporosis

Osteoporosis was induced over a four month period through ovariectomy (OVX), dietary deficiency, and steroid administration (**Figure 4A**). To verify successful induction, DXA scans were performed pre- and post-induction. It was confirmed that ovariectomized animals demonstrated a statistically significant 19% decrease in Bone Mineral Density (BMD) within the lumbar spine (**Figure 4B, 4C**) by four month post-OVX. This result was consistent with current standards for successful osteoporosis induction in sheep (43).

Successful implantation surgery

Next, implantation was performed via balloon kyphoplasty in the six sheep most susceptible to induction. Sheep were randomly implanted with the control vehicle, comprised of hyaluronic acid, hydroxyapatite, and β -TCP alone or rhNELL-1 protein lyophilized onto β -TCP (**Figure 5**). Post-surgery, animals recovered fully with no complication.

Two doses of rhNELL-1 were used (0.9 mg and 2.25 mg). Animals' vertebral bone mineral density was assessed monthly by DXA for three months post-implantation. Results revealed that rhNELL-1 treatment with either 0.9 or 2.25 mg exhibited a significant increase in BMD in comparison to control (**Figure 6**). A statistically significant difference was most apparent at two months post-implantation ($*p = 0.027$, $**p = 0.007$). By three months, a persistent increase in BMD was appreciated at the higher dose of 2.25 mg rhNELL-1 treatment ($*p = 0.047$). In summary, analysis of DXA

scans showed a significant increase in BMD among rhNELL-1 based balloon kyphoplasty specimens in comparison to control. (**Figure 6**)

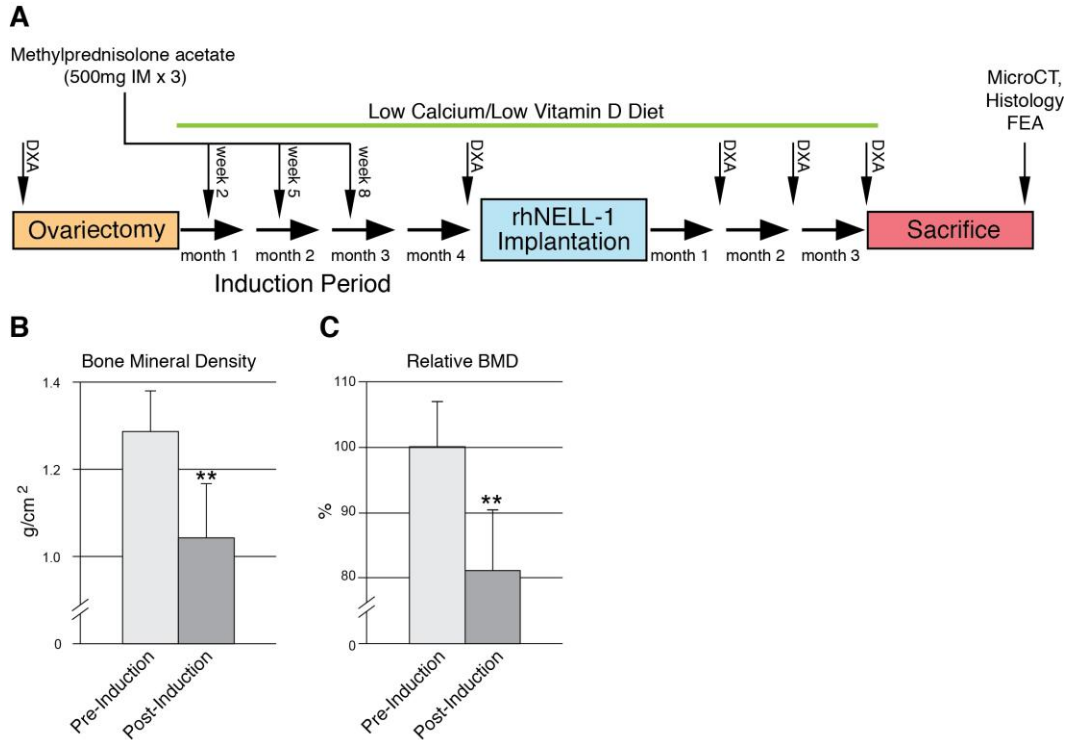





Figure 4. Induction of osteoporosis in sheep. (A) Timeline of osteoporosis induction in sheep. Osteoporosis was induced by combination of treatment with ovariectomy, steroid injection, and low calcium/low vitamin D diet. Pre- and post-induction DXA scans were performed. Post-implantation of rhNELL-1 treatment materials, DXA scans were performed monthly until sacrifice at three months, after which microCT, histological analysis and FEA was performed. (B) DXA imaging performed post-induction showed a significant decrease in Bone Mineral Density (BMD) within the sheep lumbar spine. N=8 sheep in total. (C) Ovariectomized animals demonstrated a significant percentage decrease in Bone Mineral Density (BMD) that indicated successful osteoporosis induction.

Treatment	# Vertebrae Implanted	Hyaluronic Acid (mL)	β -TCP (mg)	Hydroxyapatite (g)	Total Volume (mL)	Total Dose rhNELL-1 (mg)	Concentration rhNEL-1 (mg/mL)
Control 	6	1.1	150	1.3	1.5	0	0
rhNELL-1 (low dose) 	3	1.1	150	1.3	1.5	0.9	0.6
rhNELL-1 (high dose) 	3	1.1	150	1.3	1.5	2.25	1.5

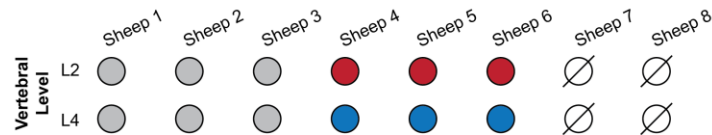


Figure 5. RhNELL-1 implant material contents and bi-level sheep balloon kyphoplasty surgery. Surgery was performed four months post-OVX on 6 mature osteoporotic sheep that were most responsive to osteoporosis induction as confirmed by DXA. The table shows rhNELL-1 implant material contents of sheep balloon kyphoplasty. The schematic illustrates a bi-level surgery of sheep vertebrae. 0.09mg of rhNELL-1 was implanted in L2 (N=3), and 2.25mg of rhNELL-1 was implanted in L4 (N=3) randomly selected sheep. Control vehicles (N=6) were implanted in L2 and L4 vertebrae of the remaining 3 sheep. L2 and L4 of sheep vertebrae are anatomically similar to human vertebrae as previously shown. Additionally, L2 and L4 are anatomically similar to each other.

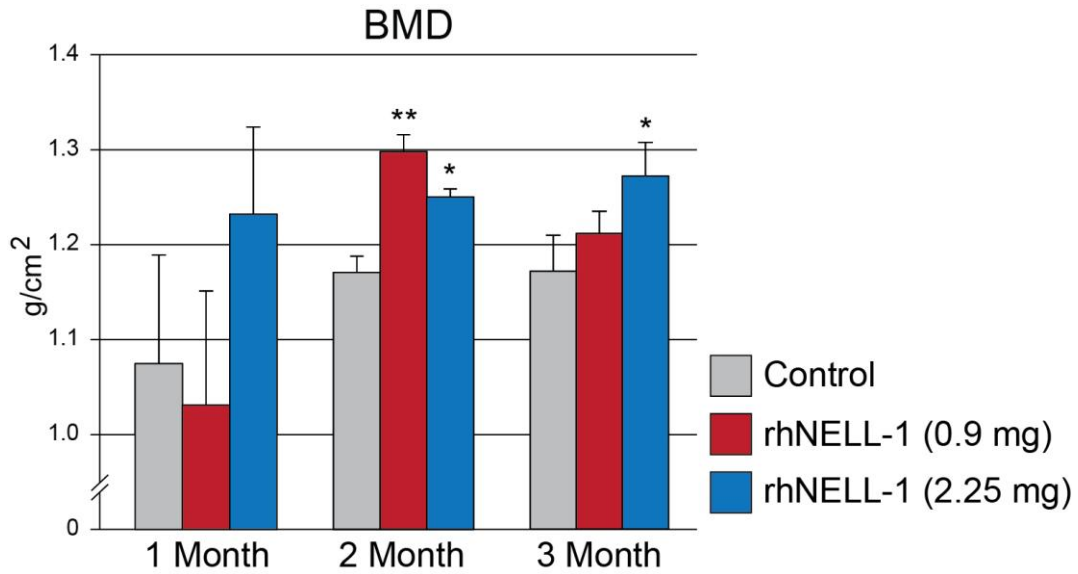


Figure 6. BMD quantification in sheep lumbar vertebrae. DXA Scans were performed at one, two, and three months after balloon kyphoplasty. Quantification of Bone Mineral Density (BMD) between control, rhNELL-1 (0.9 mg), and rhNELL-1 (2.25 mg) groups was performed. DXA scans showed a significant increase in BMD with rhNELL-1 based balloon kyphoplasty in comparison to control treatment. N=3 lumbar vertebrae per dose rhNELL-1, N=6 control-treated lumbar vertebrae. * $p < 0.05$, ** $p < 0.01$ in comparison to control at corresponding time point.

MicroCT analysis

We next sought to delineate the effects of rhNELL-1 on either cortical or cancellous bone using high-resolution microCT scans. This allowed for the high-resolution analysis of three-dimensional trabecular bone structure. Axial and sagittal images of microCT scans showed significant bone formation in rhNELL-1 based balloon kyphoplasty groups (Figure 7A).

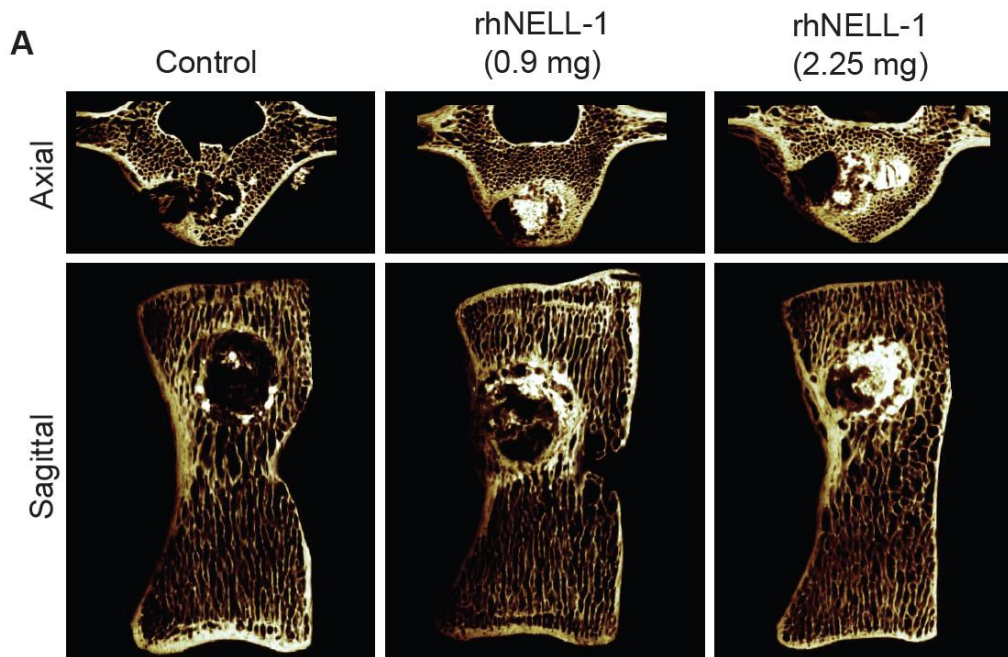


Figure 7. MicroCT analysis of sheep lumbar vertebrae.

(A) Representative microCT axial and sagittal reconstructions of sheep vertebrae treated with control, rhNELL-1 (0.9mg) and rhNELL-1 (2.25mg) balloon kyphoplasty.

Next, trabecular bone analyses were performed, and revealed a significant dose-dependent increase in BMD with rhNELL-1 treatment when compared to control (**Figure 7B**). Quantifications for fractional Bone Volume (BV/TV) was subsequently calculated, and revealed to be significantly increased with rhNELL-1 treatment at both 0.9 and 2.25 mg dosages (**Figure 7C**). Although no significant difference in Trabecular Thickness (Tb. Th) were noted (**Figure 7D**) between treatment groups and control, significantly improvements were observed in Trabecular Number (Tb. N) of both rhNELL-1-treated groups (0.9 mg and 2.25 mg) (**Figure 7E**). Additionally, a significant decrease in Trabecular Spacing (Tb. Sp) was observed in the high dose rhNELL-1 treated treatment groups to control (**Figure 7F**). In summary, microCT analysis exhibited a significant and dose-dependent increase in bone and trabecular bone quantitative measurements.

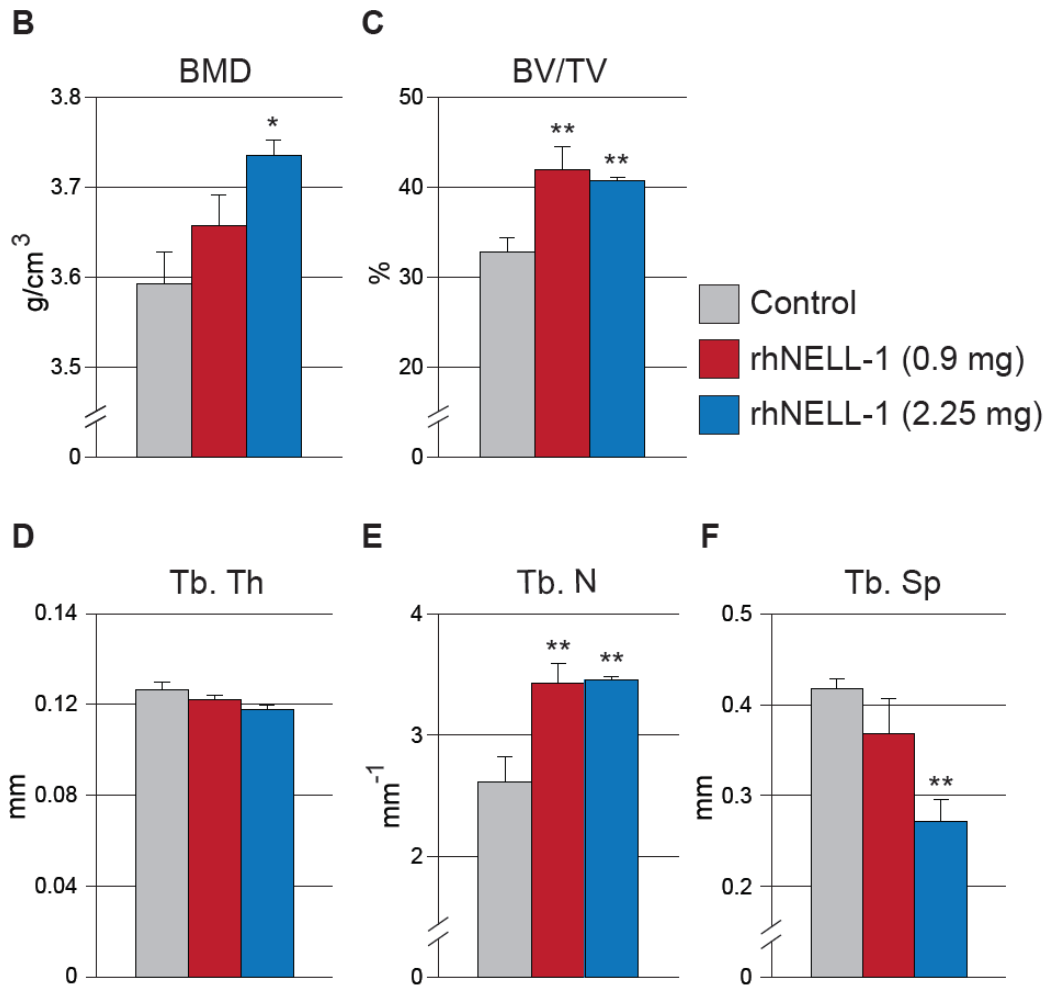


Figure 7. MicroCT analysis of sheep lumbar vertebrae. After 3 months, microCT analysis was performed including: **(B)** Bone Mineral Density (BMD), **(C)** Fractional Bone Volume (BV/TV), **(D-F)** trabecular bone measurements including, **(D)** Trabecular Thickness (Tb. Th), **(E)** Trabecular Number (Tb. N), and **(F)** Trabecular Bone Spacing (Tb. Sp). N=3 lumbar vertebrae per dose rhNELL-1, N=6 control-treated lumbar vertebrae. * $p < 0.05$, ** $p < 0.01$ in comparison to balloon kyphoplasty control.

Histological and histomorphometric analyses

Next, histology was performed on serial sections of balloon kyphoplasty implant sites to verify radiographic findings. In agreement to radiographic results, it was observed that spines treated with rhNELL-1 exhibited a significant and dose-dependent increase in bone formation in comparison to vehicle control implantation. Von Kossa MacNeal's Tetrachrome staining of the implant sites also demonstrated an increase in cancellous bone formation, in comparison to the control (**Figure 8A**).

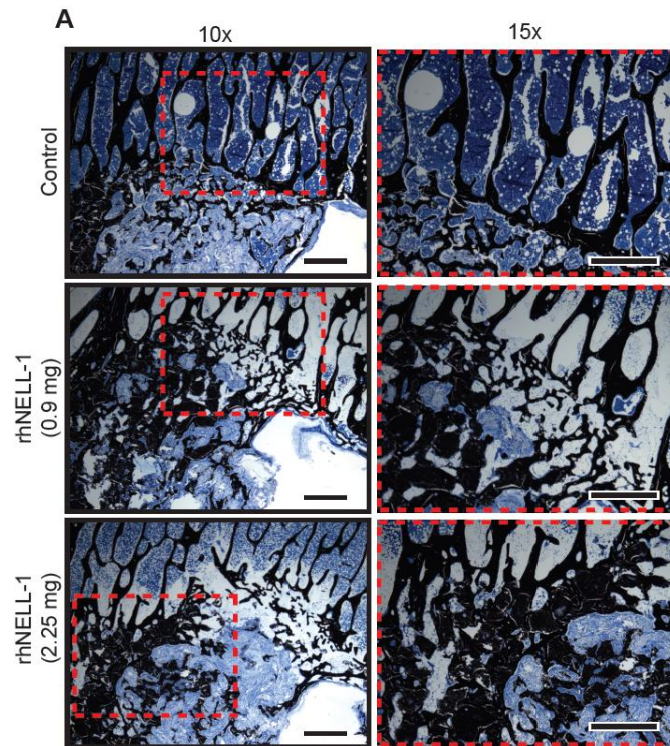


Figure 8. Histological analysis of sheep lumbar vertebrae.
 (A) Representative images of Von Kossa McNeal's Tetrachrome staining of sheep lumbar vertebral bodies were taken at peri-implant sites treated with control, rhNELL-1 (0.9 mg) and rhNELL-1 (2.25 mg).

Histomorphometric analysis further confirmed the observed significant differences in bone formation. First, Cortical Width (Ct. Wi) quantifications of serial sections exhibited a significant and dose-dependent increase between rhNELL-1 treated groups in comparison to control. In both dosages, the rhNELL-1 treated group exhibited greater and thicker endocortical bone formation than the control treated group (**Figure 8B**). Next, cancellous bone was analyzed. Both rhNELL-1-treated groups exhibited a greater percentage of Trabecular Bone Area (% Tb. Ar) in comparison to the control group (**Figure 8C**). However, there was no significant difference in Trabecular Width (Tb. Wi) between treatment and control groups (**Figure 8D**). When comparing Trabecular Number (Tb. N), a significant increase was observed between rhNELL-1 treated groups in comparison to the control (**Figure 8E**). Lastly, we investigated Trabecular Spacing (Tb. Sp), whereby a significant and dose-dependent decrease was observed, suggesting dense cancellous bone formation with rhNELL-1 treatment (**Figure 8F**). Thus and in summary, histologic and histomorphometric measurements confirmed initial finding radiographic findings that rhNELL-1 treatment, dose-dependantly, improves bone formation in osteoporotic sheep.

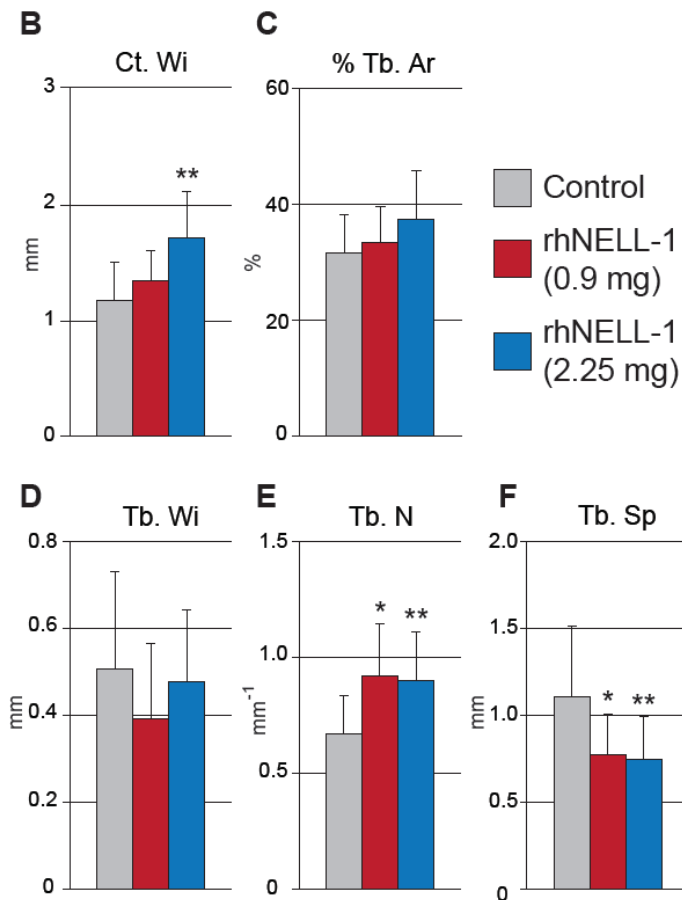


Figure 8. Histological analysis of sheep lumbar vertebrae. (B-F) Histomorphometric quantification using Von Kossa McNeal's Tetrachrome stained slides of samples treated with control, rhNELL-1 (0.9 mg) and rhNELL-1 (2.25 mg) balloon kyphoplasty. Bone measurements include: **(B)** Cortical Width (Ct. Wi), **(C)** Percent Trabecular Bone (% Tb. Ar), **(D)** Trabecular Width (Tb. Wi), **(E)** Trabecular Number (Tb. N), and **(F)** Trabecular Bone Spacing (Tb. Sp). N=3 lumbar vertebrae per dose rhNELL-1, N=6 control-treated lumbar vertebrae. * $p < 0.05$ and ** $p < 0.01$ in comparison to balloon kyphoplasty control.

As increased trabecular bone with rhNELL-1 could be attributable to either increased bone formation, reduced bone resorption, or a combination of the two processes, we next examined osteoblasts and osteoclasts through histological analysis. Osteoblasts and osteoclast number were quantified in the peri-implant site tissue by examining cells for characteristic morphology (**Figure 9**). Results revealed that Osteoblast Number (Ob. N) per 200x field was significantly increased in the high dose rhNELL-1 group in comparison to the control group (**Figure 9A**). Osteoblast number was determined by characteristic cuboidal morphology in bone-lining cells. In contrast, Osteoclast Number (Oc. N) per 200x field showed a significant and dose-dependent decrease with rhNELL-1 treatment groups (**Figure 9B**). Osteoclast number was defined as the number of TRAP (Tartrate Resistant Acid Phosphatase) positive, multi-nucleated, bone-lining cells. In summary, rhNELL-1 treatment by balloon kyphoplasty resulted in a dose-dependent increase in osteoblast expression with marked decreases in osteoclast cell number.

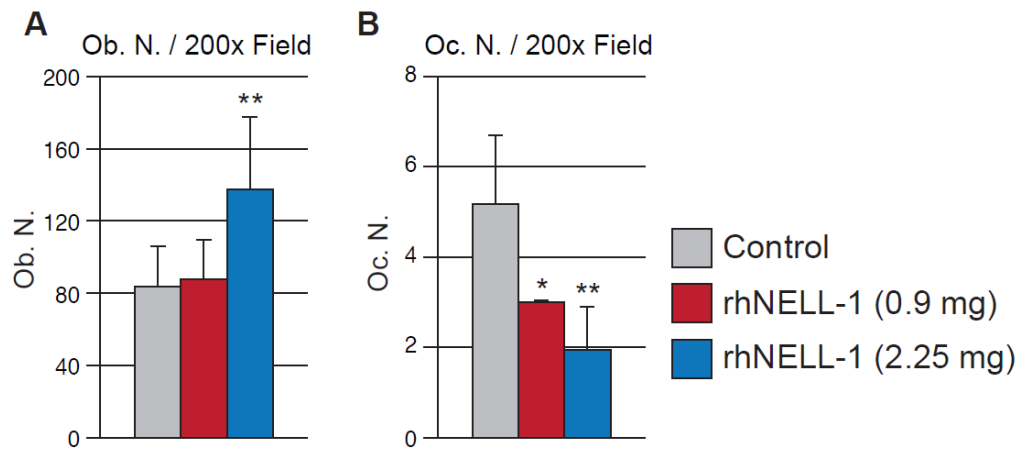


Figure 9. Osteoblast and Osteoclast numbers in the peri-implant bone tissue. (A) Quantification of Osteoblast Number obtained from N=16 random histological fields (200x) per treatment group (Ob. N / 200x Field). (B) Quantification of Osteoclast Number obtained from N=12 random histological fields (200x) per treatment groups (Oc. N / 200x Field). N=3 lumbar vertebrae per dose rhNELL-1, N=6 control-treated lumbar vertebrae. * $p < 0.05$, ** $p < 0.01$ in comparison to balloon kyphoplasty control.

Biomechanical analysis

Lastly, biomechanical properties of treated spines were assessed using non-destructive, computerized, finite element analysis (FEA). Strain energy is defined as the energy absorbed by a system undergoing deformations. Trabecular bone positioned 0.5 mm caudal to the implant site in the midline of the vertebrae and spanning a 5mm x 10mm x 5 mm was selected as the region of interest for the FEA model to best simulate compress stress stain post loading. FEA studies revealed decreased strain energy among rhNELL-1 treatment groups in comparison to control. A significant decrease in total strain energy was observed across both rhNELL-1 treatment groups in comparison to control (**Figure 10B**). Next, compressive stress values of treatment groups were visualized (**Figure 10C**). Specimens with rhNELL-1 treatment exhibited similar compressive stress strains, ranging from 0.1 MPa (blue) to 0.5 MPa (cyan), compared to control-treated animals, which exhibited relatively higher compressive stress strain, ranging from from 0.1 MPa (blue) to 1.5 MPa (green). In summary, FEA demonstrated that rhNELL-1 based balloon kyphoplasty resulted in a more compressive stress-resistant composition in comparison to control.

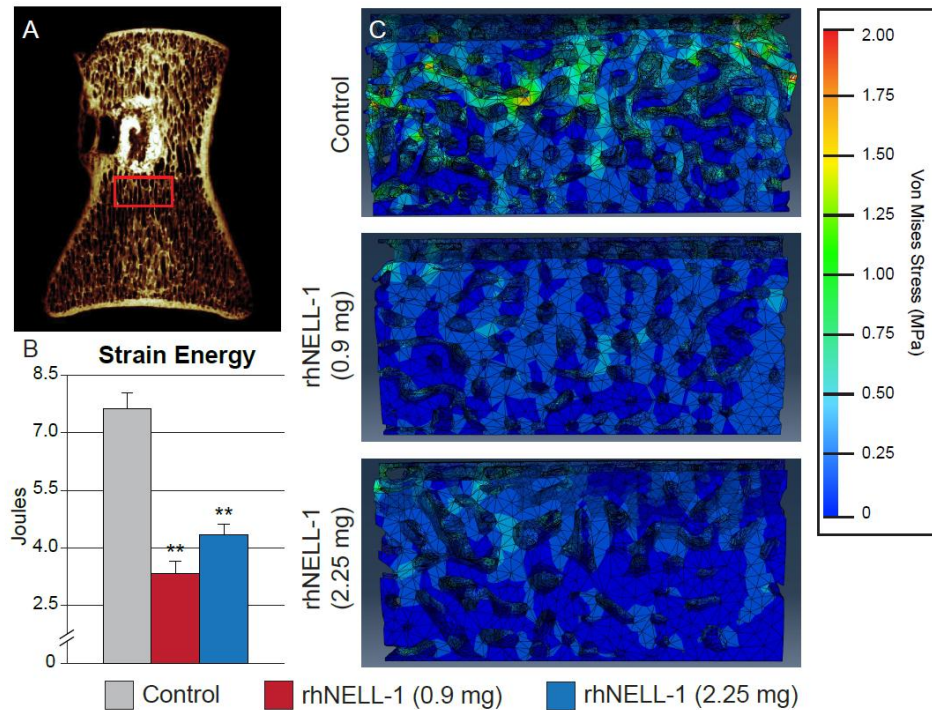


Figure 10. Finite Element Analysis of peri-implant trabecular bone. (A) Region of Interest (ROI) for biomechanical testing using Finite Element Analysis (FEA). A coronal microCT reconstruction image shows the the area of trabecular bone positioned 0.5 mm caudal to the implant site in the midline of the vertebrae and spanning a 5mm x 10mm x 5 mm ROI. (B) Total strain energy determined by finite element analysis. (C) Representative images of FEA models showing stressed elements post loading. High strain areas are indicated with yellow/green. N=3 lumbar vertebrae per dose rhNELL-1, N=6 control-treated lumbar vertebrae. * $p < 0.05$, ** $p < 0.01$ in comparison to balloon kyphoplasty control.

DISCUSSION

In the present study, our findings suggest that exogenous rhNELL-1 protein application via balloon kyphoplasty led to an improvement in bone quality in osteoporotic sheep model, as evaluated by radiographic, histological, and biomechanical analyses. RhNELL-1 treatment was found to increase both cortical and cancellous bone in the lumbar vertebrae. Finite element analysis suggested an increase in the structural stability and resistance to compressive stress with rhNELL-1 treatment. Finally, an increase in osteoblast : osteoclast number was observed with rhNELL-1 delivery. This evidence demonstrated that rhNELL-1 plays a role as an anabolic as well as an anti-resorptive agent for improved bone quantity and bone quality in this model.

On a cellular level, osteoporosis can be attributed to the imbalance between bone formation and bone resorption (49). This occurs due to a reduction in osteoblast number and activity, as well as an increase in osteoclast number and activity (50). NELL-1 has previously been published suggesting its role as a positive regulator of osteoblastogenesis and bone deposition via Runx2 and MAPK signaling pathways. NELL-1 operates as a downstream mediator of Runx2, a key factor in osteogenic differentiation, and the upregulation of Runx2 via NELL-1 occurs by enhancement of its phosphorylation through activation of MAPK signaling (38). However, the exact mechanisms for NELL-1's negative effects on bone resorption have yet to be fully understood. One possibility for this is via the canonical Wnt signaling pathway, which is known to enhance osteoprogenitor cell proliferation and osteoblastogenesis while also having anti-osteoclast activity (51). Ongoing studies are examining the potential intersection

between NELL-1 and Wnt-signaling. Nonetheless, NELL-1 has promising results at combating osteoporosis by decreasing bone resorption and increasing bone formation.

The present study's main implication is that rhNELL-1 based material may be a new potentially preferable bone graft substitute. Furthermore, rhNELL-1 is a promising efficacious therapy in the setting of osteoporosis. Presently, therapeutic options for osteoporotic patients with VCF's are limited to bone grafts or polymethyl methacrylate (PMMA) balloon kyphoplasty. Nonetheless, autologous bone grafting remains the gold standard for bone repair (52), though possessing significant disadvantages, including donor site morbidity (53), complications due to extended operating time and limited supply of host bone (54). To combat these issues, growth factor-based therapies were studied, the only of which is FDA approved is Bone Morphogenic Protein 2 (BMP2) (INFUSE ® Bone Graft). Although showing promising osteoinductive properties, BMP2 acts as a direct stimulant of osteoclastic bone resorption (55), which can lead to complications such as vertebral collapse or additional fractures. Thus, caution must be exercised when implementing BMP2-based therapies. Alternately, PMMA balloon kyphoplasty has been increasingly adopted for the treatment of osteoporotic compression fracture (56). However, as mentioned PMMA has several associated potential risks. Polymethyl methacrylate is not bioabsorbable and its unreacted monomer is toxic. Additionally, it has high polymerization temperatures (16) and its high stiffness causes a biomechanical mismatch between treated and untreated vertebral levels, leading to adjacent-level fractures (18). In contrast, no previous studies have reported NELL-1 to be toxic or have any other associated adverse effects. Finally, rhNELL-1 lyophilized on a

porous and resorbable β -Tricalcium phosphate (β -TCP) scaffold with hydroxyapatite coating allows better interaction with host bone. It increases both, the biochemical stability as well as the bioavailability of rhNELL-1 for protein delivery (57). Together with our results, rhNELL-1 is a promising future component of a bone graft substitute for treatment in the setting of osteoporosis.

In summary, we have found that treatment with implantation of rhNELL-1 and TCP prevented further resorption of bone and increased regeneration of bone in the setting of osteoporosis in sheep. RhNELL-1 balloon kyphoplasty successfully induced an increase in osteoblast number and conversely a decrease in osteoclast number resulting in improved cortical and cancellous bone regeneration in osteoporotic sheep spine. Therefore, rhNELL-1 balloon kypholasty represents a potential new anabolic, anti-resorptive local therapy for treating osteoporotic bone loss and/or fractures, specifically in the setting of vertebral compression fractures.

References:

1. Barr JD, Barr MS, Lemley TJ, McCann RM. Percutaneous vertebroplasty for pain relief and spinal stabilization. *Spine* 15;25(8):923-8. 2000.
2. Riggs BL, Melton LJ, 3rd. The worldwide problem of osteoporosis: insights afforded by epidemiology. *Bone*.17:505S-11S. 1995.
3. Melton LJ 3rd. Epidemiology of spinal osteoporosis. *Spine* 15;22(24 Suppl):2S-11S 1997.
4. Leidig G, Minne HW, Sauer P, Wuster C, Wuster J, Lojen M, et al. A study of complaints and their relation to vertebral destruction in patients with osteoporosis. *Bone Miner*.8:217-29. 1990.
5. Mathis JM, Petri M, Naff N. Percutaneous vertebroplasty treatment of steroid-induced osteoporotic compression fractures. *Arthritis Rheum*.41:171-5. 1998.
6. Lyles KW, Gold DT, Shipp KM, Pieper CF, Martinez S, Mulhausen PL. Association of osteoporotic vertebral compression fractures with impaired functional status. *Am J Med*. 94:595-601. 1993.
7. Cauley JA, Thompson DE, Ensrud KC, Scott JC, Black D. Risk of mortality following clinical fractures. *Osteoporos Int*. 11:556-61. 2000.
8. Schlaich C, Minne HW, Bruckner T, Wagner G, Gebest HJ, Grunze M, et al. Reduced pulmonary function in patients with spinal osteoporotic fractures. *Osteoporos Int*.8:261-7. 1998.
9. Gold DT. The clinical impact of vertebral fractures: quality of life in women with osteoporosis. *Bone*. 18(3 Suppl):185S-189S. 1996.

10. Moerman EJ, Teng K, Lipschitz DA, Lecka-Czernik B. Aging activates adipogenic and suppresses osteogenic programs in mesenchymal marrow stroma/stem cells: the role of PPAR-gamma2 transcription factor and TGF-beta/BMP signaling pathways. *Aging Cell*.3:379-89. 2004.
11. Egermann M, Schneider E, Evans CH, Baltzer AW. The potential of gene therapy for fracture healing in osteoporosis. *Osteoporos Int*. 16 Suppl 2:S120-8. 2005.
12. Robinson Y, Olerud C. Vertebroplasty and kyphoplasty--a systematic review of cement augmentation techniques for osteoporotic vertebral compression fractures compared to standard medical therapy. *Maturitas*.72:42-9. 2012.
13. Cloft HJ, Jensen ME. Kyphoplasty: an assessment of a new technology. *AJNR Am J Neuroradiol*.28:200-3. 2007.
14. Robinson Y, Heyde CE, Forsth P, Olerud C. Kyphoplasty in osteoporotic vertebral compression fractures--guidelines and technical considerations. *J Orthop Surg Res*.6:43. 2011.
15. Taylor RS, Fritzell P, Taylor RJ. Balloon kyphoplasty in the management of vertebral compression fractures: an updated systematic review and meta-analysis. *Eur Spine J*.16:1085-100. 2007.
16. Deramond H, Wright NT, Belkoff SM. Temperature elevation caused by bone cement polymerization during vertebroplasty. *Bone*. 25:17S-21S. 1999.
17. Nussbaum DA, Gailloud P, Murphy K. A review of complications associated with vertebroplasty and kyphoplasty as reported to the Food and Drug Administration medical device related web site. *J Vasc Interv Radiol*.15:1185-92. 2004.

18. Fribourg D, Tang C, Sra P, Delamarter R, Bae H. Incidence of subsequent vertebral fracture after kyphoplasty. *Spine*.29:2270-6; discussion 7. 2004.
19. Le Nihouannen D, Daculsi G, Saffarzadeh A, Gauthier O, Delplace S, Pilet P, et al. Ectopic bone formation by microporous calcium phosphate ceramic particles in sheep muscles. *Bone*.36:1086-93. 2005.
20. Heo HD, Cho YJ, Sheen SH, Kuh SU, Cho SM, Oh SM. Morphological changes of injected calcium phosphate cement in osteoporotic compressed vertebral bodies. *Osteoporos Int*.20:2063-70. 2009.
21. Zhang X, Zara J, Siu RK, Ting K, Soo C. The role of NELL-1, a growth factor associated with craniosynostosis, in promoting bone regeneration. *J Dent Res*.89:865-78. 2010.
22. Aghaloo T, Cowan CM, Chou YF, Zhang X, Lee H, Miao S, et al. Nell-1-induced bone regeneration in calvarial defects. *Am J Pathol*.169:903-15. 2006.
23. Li W, Lee M, Whang J, Siu RK, Zhang X, Liu C, et al. Delivery of lyophilized Nell-1 in a rat spinal fusion model. *Tissue Eng Part A*.16:2861-70. 2010.
24. Siu RK, Lu SS, Li W, Whang J, McNeill G, Zhang X, et al. Nell-1 protein promotes bone formation in a sheep spinal fusion model. *Tissue Eng Part A*.17:1123-35. 2011.
25. Lu SS, Zhang X, Soo C, Hsu T, Napoli A, Aghaloo T, et al. The osteoinductive properties of Nell-1 in a rat spinal fusion model. *Spine J*. 7:50-60. 2007.
26. Li W, Zara JN, Siu RK, Lee M, Aghaloo T, Zhang X, et al. Nell-1 enhances bone regeneration in a rat critical-sized femoral segmental defect model. *Plast Reconstr Surg*.127:580-7. 2011.

27. Riew KD, Wright NM, Cheng S, Avioli LV, Lou J. Induction of bone formation using a recombinant adenoviral vector carrying the human BMP-2 gene in a rabbit spinal fusion model. *Calcif Tissue Int.*63:357-60. 1998.
28. Poynton AR, Lane JM. Safety profile for the clinical use of bone morphogenetic proteins in the spine. *Spine.*27:S40-8. 2002.
29. Haid RW, Jr., Branch CL, Jr., Alexander JT, Burkus JK. Posterior lumbar interbody fusion using recombinant human bone morphogenetic protein type 2 with cylindrical interbody cages. *Spine J.*4:527-38; discussion 38-9. 2004.
30. Shields LB, Raque GH, Glassman SD, Campbell M, Vitaz T, Harpring J, et al. Adverse effects associated with high-dose recombinant human bone morphogenetic protein-2 use in anterior cervical spine fusion. *Spine.*31:542-7. 2006.
31. Smucker JD, Rhee JM, Singh K, Yoon ST, Heller JG. Increased swelling complications associated with off-label usage of rhBMP-2 in the anterior cervical spine. *Spine.*31:2813-9. 2006.
32. Perri B, Cooper M, Lauryssen C, Anand N. Adverse swelling associated with use of rh-BMP-2 in anterior cervical discectomy and fusion: a case study. *Spine J.*7:235-9. 2007.
33. Vaidya R, Carp J, Sethi A, Bartol S, Craig J, Les CM. Complications of anterior cervical discectomy and fusion using recombinant human bone morphogenetic protein-2. *Eur Spine J.*16:1257-65. 2007.
34. Tumialan LM, Pan J, Rodts GE, Mummaneni PV. The safety and efficacy of anterior cervical discectomy and fusion with polyetheretherketone spacer and

- recombinant human bone morphogenetic protein-2: a review of 200 patients. *J Neurosurg Spine*.8:529-35. 2008.
35. Zara JN, Siu RK, Zhang X, Shen J, Ngo R, Lee M, et al. High doses of bone morphogenetic protein 2 induce structurally abnormal bone and inflammation in vivo. *Tissue Eng Part A*.17:1389-99. 2011.
36. James AW, Pan A, Chiang M, Zara JN, Zhang X, Ting K, et al. A new function of Nell-1 protein in repressing adipogenic differentiation. *Biochem Biophys Res Commun*.411:126-31. 2011.
37. Zhang X, Ting K, Bessette CM, Culiati CT, Sung SJ, Lee H, et al. Nell-1, a key functional mediator of Runx2, partially rescues calvarial defects in Runx2(+/-) mice. *J Bone Miner Res*.26:777-91. 2011.
38. Bokui N, Otani T, Igarashi K, Kaku J, Oda M, Nagaoka T, et al. Involvement of MAPK signaling molecules and Runx2 in the NELL1-induced osteoblastic differentiation. *FEBS Lett*.582:365-71. 2008.
39. Reid JE, Meakin JR, Robins SP, Skakle JM, Hukins DW. Sheep lumbar intervertebral discs as models for human discs. *Clin Biomech (Bristol, Avon)*.17:312-4. 2002.
40. Turner AS. The sheep as a model for osteoporosis in humans. *Vet J*.163:232-9. 2002.
41. US Dept of Health and Human Services PHS, NIH. Committee on Care and Use of Laboratory Animals of the ILAR. 1985.

42. Gaynor JS, Monnet E, Selzman C, Parker D, Kaufman L, Bryant HU, et al. The effect of raloxifene on coronary arteries in aged ovariectomized ewes. *J Vet Pharmacol Ther.*23:175-9. 2000.
43. Zarrinkalam MR, Beard H, Schultz CG, Moore RJ. Validation of the sheep as a large animal model for the study of vertebral osteoporosis. *Eur Spine J.*18:244-53. 2009.
44. Karasik D, Hsu YH, Zhou Y, Cupples LA, Kiel DP, Demissie S. Genome-wide pleiotropy of osteoporosis-related phenotypes: the Framingham Study. *J Bone Miner Res.*25:1555-63. 2010.
45. Honig S, Chang G. Osteoporosis: An update. *Bulletin of the NYU Hospital for Joint Diseases.* 70(3):140-4. 2012.
46. Parfitt AM, Drezner MK, Glorieux FH, Kanis JA, Malluche H, Meunier PJ, et al. Bone histomorphometry: standardization of nomenclature, symbols, and units. Report of the ASBMR Histomorphometry Nomenclature Committee. *J Bone Miner Res.*2:595-610. 1987.
47. Cheung JT, Zhang M, Chow DH. Biomechanical responses of the intervertebral joints to static and vibrational loading: a finite element study. *Clin Biomech.*18:790-9. 2003.
48. Kuo CS, Hu HT, Lin RM, Huang KY, Lin PC, Zhong ZC, et al. Biomechanical analysis of the lumbar spine on facet joint force and intradiscal pressure--a finite element study. *BMC Musculoskelet Disord.*11:151. 2010.
49. Teitelbaum SL. Bone resorption by osteoclasts. *Science.*289:1504-8. 2000.

50. Marie PJ. Osteoporosis: a disease of bone formation. *Medicographia*.32:10-6. 2010.
51. Yavropoulou MP, Yovos JG. The role of the Wnt signaling pathway in osteoblast commitment and differentiation. *Hormones (Athens)*.6:279-94. 2007.
52. Laurencin C, Khan Y, El-Amin SF. Bone graft substitutes. *Expert Rev Med Devices*.3:49-57. 2006.
53. Laurie SW, Kaban LB, Mulliken JB, Murray JE. Donor-site morbidity after harvesting rib and iliac bone. *Plast Reconstr Surg*.73:933-8. 1984.
54. Frodel JL, Jr., Marentette LJ, Quatela VC, Weinstein GS. Calvarial bone graft harvest. Techniques, considerations, and morbidity. *Arch Otolaryngol Head Neck Surg*.119:17-23. 1993.
55. Kaneko H, Arakawa T, Mano H, Kaneda T, Ogasawara A, Nakagawa M, et al. Direct stimulation of osteoclastic bone resorption by bone morphogenetic protein (BMP)-2 and expression of BMP receptors in mature osteoclasts. *Bone*.27:479-86. 2000.
56. Mathis JM, Ortiz AO, Zoarski GH. Vertebroplasty versus kyphoplasty: a comparison and contrast. *AJNR Am J Neuroradiol*.25:840-5. 2004.
57. Hu J, Hou Y, Park H, Lee M. Beta-tricalcium phosphate particles as a controlled release carrier of osteogenic proteins for bone tissue engineering. *J Biomed Mater Res A*.100:1680-6. 2012.